An IR-based methodology for indirect measurement of average inner temperatures

Elisa Carvajal Trujillo[a], Francisco Jiménez Espadafor Aguilar[a], Ricardo Chacartegui-Ramírez[a]

[a] Universidad de Sevilla, Seville, Spain ecarvajal@us.es
[b] Universidad de Sevilla, Seville, Spain fcojjea@us.es
[c] Universidad de Sevilla, Seville, Spain ricardoch@us.es

Abstract:

In many thermal processes, elements with high temperatures are distributed in a non-uniform way, whose internal surface temperatures must be known. Intrusive through-wall sensors are commonly used, but this technique is not possible in some cases. In addition, it requires numerous sensors distributed over the entire surface to know the temperature of the entire surface adequately. This is the case with the inner surfaces of the cylinder and cylinder head of reciprocating internal combustion engines, where it is relatively easy to measure the external temperature of the surfaces but not the temperature distribution of the inner surfaces. The accurate evaluation of this interior temperature is relevant for the determination of inner processes, such as the rejected heat from the combustion chamber.

In this work, a methodology for the estimation of the average temperature of the interior surfaces of elements is presented. Starting from the experimental measurement of the temperature distribution of the exterior surfaces and measuring the total energy transferred from the interior to the exterior surface, the proposed methodology uses an iterative sequence of simulations using finite element methods. The result is a distribution of temperatures on the interior surfaces, whose average temperature is taken as the temperature of the interior surfaces. The minimum mean square error (MSE) value achieved is of the order of 50. The method converges when an improvement of the MSE by less than 5% is achieved. The convective heat transfer coefficients from the finned surface to the atmosphere is $1{,}4 \cdot 10^{-4}$ W/mm^{2}K, which are normal values associated with natural convection.

This methodology has been validated by building a prototype in the laboratory. The methodology has achieved a high agreement between the measured and the predicted values.

Keywords:

Sensors, Infrared thermal images, thermal engine, temperature indirect measurement

1. Introduction

In thermal systems that are composed of mechanisms and thermal generation within them, the prediction of heat transfer is important as it influences heat losses. An accurate prediction of heat losses are essential to know the performance, power, emissions and stress field [1]. Examples of such systems are heat engines, such as reciprocating internal combustion engines, or thermal storage systems based on thermochemical reactions. Knowing the temperature distribution inside these systems is important to characterise the behaviour of these thermal systems.

Measuring the interior temperatures of walls that are not accessible is quite costly and difficult. Intrusive techniques are normally used, with holes drilled to install the sensors, which can modify the phenomenon and render the model useless [2]. Measurements based on optical techniques are also common [3] but require specific windows or special preparation of the model to be measured, with optical access. An example would be the diode laser sensor [4] or coherent anti-Stokes Raman spectroscopy [5].

Directly measuring temperatures on indoor surfaces using sensors can be complicated and intrusive [6]. In addition, the spatial variation of temperatures on indoor surfaces is important [7,8]. If the measurement is reduced to a few points, the averages can be non-representative of the whole assembly. Moreover, it is challenging for small systems to install a relevant number of sensors on the inner surfaces, with the risk of affecting inner flows. This is especially important for measuring the inner surface of combustion chambers of reciprocating internal combustion engines or high-temperature energy storage systems where the gas temperature could be considered constant for many analyses, but for the purpose of mechanical calculations and heat transfer calculations, the assumption of constant surface temperature is not valid. The smaller the

https://doi.org/10.52202/069564-0035

volume and the higher the temperature, the more complicated the installation and the more intrusive the measurement method.

In addition, when the outer surface of the system whose inner surface temperature is to be measured is not uniform, for instance, air cooling internal combustion engines with an external finned surface, measurement becomes even more difficult due to the more difficult installation conditions of the sensors.

There are indirect methods for the determination of these temperatures based on heat transfer mechanisms. Some authors use resistance-capacitance models [9]. Other authors use models that solve by finite element methods, in stationary or transient regimes. For both types of models, the boundary conditions are varied: constant temperatures on the inner and outer surface, constant heat transfer coefficients on the inner wall and temperature of the outer wall equal to that of the coolant or heat transfer coefficients in different areas of the outer surface of the piston [10, 11, 12].

It should also be noted that the derivation of the values of the boundary conditions for these simulations is varied. In many cases, the authors use values of conditions from the literature, which do not ensure their validity if extrapolated to different engines or systems. Other authors obtain these values through previous simulations of the combustion cycle or the internal process within the system. Obtaining accurate boundary condition values from experimental measurements is challenging [13].

In general, the most usual boundary condition for the outer surface side is to impose either the surface temperatures, the heat transfer coefficient or the coolant temperature. In the literature, most of the studies applied to internal combustion engines are directed to the study of water-cooled systems, in which the water temperature is almost constant or varies slightly, and the outer surfaces are smooth and do not have extended surfaces, unlike the case of air cooling. This work presents a methodology for an accurate evaluation of the inner temperature of high-temperature thermal energy systems. It is a non-intrusive methodology, requiring only infrared imaging, measurement or estimation of total heat and the use of CFD software for heat transfer analysis. Unlike other methodologies, no contact or drilling is required for thermocouple or heat flow meter placement. It is developed for being applied to hard-to-monitor systems, such as internal combustion engines or high-temperature energy storage systems. The methodology is demonstrated in an air-cooled internal combustion engine but is fully applicable to any other thermal system with the characteristics described.

2. Preliminary considerations

Several considerations have to be made before proposing a methodology for the indirect determination of the inner temperature of systems, inside which there is thermal generation or gases at high temperatures and cannot be accessed by simple methods. These considerations are related to the use of the finite element method (FEM), appropriate selection of the boundary conditions, analysis of the theoretical basis of heat transfer through extended surfaces; available experimental techniques; election of the resolution method and setting of admissible errors.

2.1. Application of the finite element method to problems in conduction and convection heat transfer

The following steps are required to solve a thermal problem using FEM:

- Phase 1 "Preprocessing": meshing, development of the equations for each element, creation of the total conductivity matrix and application of the boundary conditions and loads.
- Phase 2 "Equation solving": solving the set of linear algebraic equations to obtain the results at the nodes.
- Phase 3 "Post-processing": extraction of the information required for this research. For example, the total heat loss of a body under study or the temperature distribution on selected surfaces of this system.

Equation (1) is the form of the equations characterizing heat transfer by convection and conduction under stationary conditions:

$$[K]\{u\} = \{P\} + \{N\}, \tag{1}$$

Where [K] is the total conductivity matrix, {u} is the vector of temperatures of the nodes to be known, {P} is the vector of heat loads that are constant and {N} is the vector of nonlinear heat fluxes that depend on temperature. The vector {P} is associated with the heat transfer occurring at the surface of the element as well as the generation within the element. The vector {N} is associated with convection at the surface of the solid and temperature-dependent heat loads.

The chosen software is NC/NASTRAN and uses an iteration scheme based on the Newton-Raphson method. It is useful to follow the following two recommendations so that the iterative process can converge properly:

- Initial temperature estimation: for highly nonlinear problems, the iterative solution is very sensitive to the assumed initial temperature.

https://doi.org/10.52202/069564-0035

- Convergence criterion: the first time a problem is solved, it is advisable to keep the default values of the parameters that control the iterative process. For problems with poor convergence, it is possible to increase the values of the tolerances, although this decreases the accuracy.

2.2. Analytical resolution of heat transfer by conduction and convection of finned surfaces

As a previous step to the determination of the methodology, it is necessary to study the theoretical basis of heat transfer on extended surfaces. This study will allow us to justify the methodology and better interpret the results.

In the conduction analysis for a generic annular fin, Figure1, the following assumptions are adopted:

- One-dimensional conduction in the radial direction of the fin. If the longitudinal dimensions are much larger than the fin thickness t, then the temperature changes in the longitudinal direction are much larger than those in the transverse direction.
- Steady-state conditions.
- Constant and non-temperature-dependent conductivity.
- Radiative transfer from the fin surfaces is negligible.
- There is no energy generation in the volume considered.
- The heat transfer coefficient is constant over the entire surface.

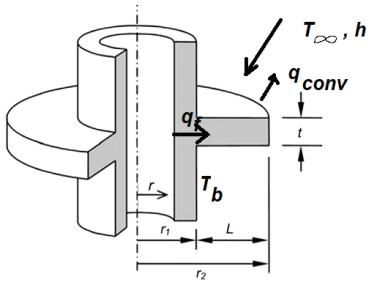

Figure. 2. Fin model and characteristic dimensions.

The conduction equation in the fin is a zero-order modified Bessel equation, Eq. (2):

$$\frac{d^2\theta}{dr} + \frac{1}{r}\frac{d\theta}{dr} - m^2\theta = 0, \tag{2}$$

where $m^2 = 2h/kt$ y $\theta = T - T_\infty$.

The temperature distribution is obtained once the boundary conditions have been chosen. The following four sets of possible boundary conditions can be applied:

- CC1, where heat arriving by conduction at the beginning of the fin is transmitted by convection along the fin;
- CC2, in which the heat arriving at the end of the fin is negligible and, therefore, the fin edge can be considered adiabatic;
- CC3, in which the temperature of the fin edge is known and;
- CC4 represents the ideal case in which the fin extension is so large that it can be considered infinite, and therefore, the temperature at the fin edge is equal to the ambient temperature.

Figure 3 illustrates the temperature distribution for an annular ring case of the inner and outer radius of 50 and 100 mm, respectively, with a heat transfer coefficient equal to 150 W/m^{2}K, the thickness of 5 mm and end temperatures of 100 ºC and 80 ºC, ambient temperature of 50 ºC. The heat fluxes for boundary conditions CC1, CC2, CC3 and CC4 are 244, 238, 230 and 387 W/m^2, respectively. As can be seen, the last boundary condition CC4 differs quite a lot from the remaining ones, as the ratio of the exterior to interior radius is not high.

Considering the objective of this work, the most appropriate boundary condition is CC1 because the transmission at the tip is by convection. However, for the characteristic dimensions of the fins, CC2 and CC3 would also be valid. The distribution can be approximated by straight lines to achieve zero errors at the base and tip of the fin.

In a first approximation, the solution for boundary conditions CC1, CC2 and CC3 can be approximated by straight lines to achieve zero errors at the base and the tip of the fin. The maximum relative approximation

error is 6.5% and occurs at the midpoint of the fin. Because these are small errors, the fins can be made independent, in terms of temperature, of the body to which they are attached.

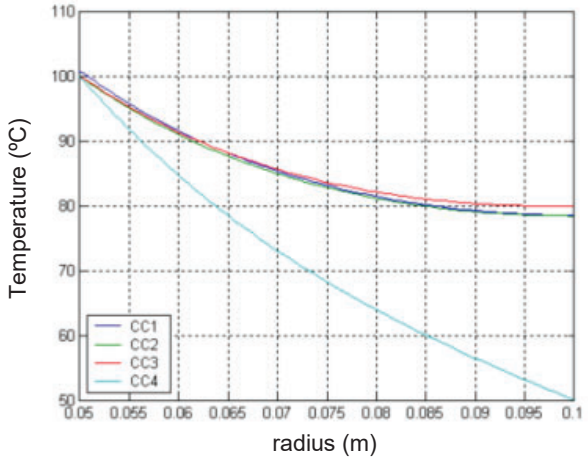

Figure. 3. Evolution of temperatures along an annular fin for different boundary conditions.

2.3. Finite element method (FEM) resolution of conduction and convection heat transfer of extended surfaces

A simple model of a trapezoidal fin is initially simulated to validate and understand the FEM resolution of heat transfer. Figure 3 shows the fin and conditions and simulation results.

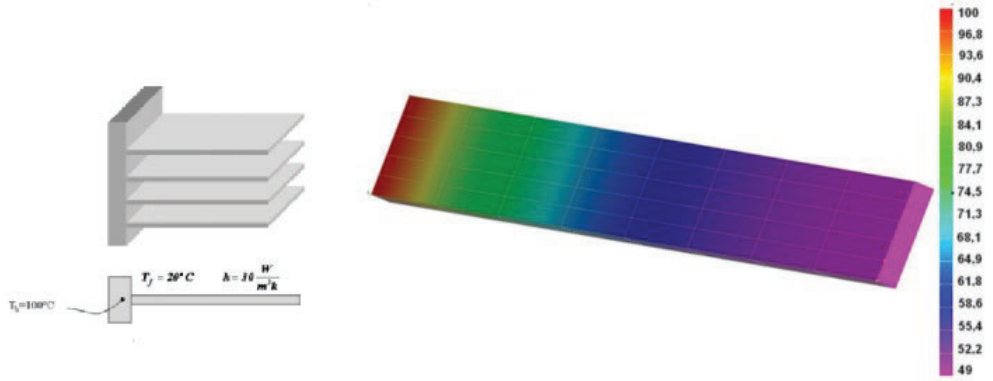

Figure. 3. a) Fin model; b) Simulation results

The temperatures obtained by analytical resolution and by FEM are compared and show divergences of less than 0,5%, which are smaller the more elements the model meshing has, although its complexity and computational load also increase.

2.4. Experimental setup

An experimental installation for the measurement of inner temperatures of systems by means of the methodology proposed in this work and for its validation is carried out., which consists of a large box, in comparison with those of the system to be tested, totally hermetic and thermally isolated from the outside. Inside this box, electrical resistors were placed. On the upper surface of the box, there is an opening in which the inner surface of the component to be tested is fitted. In this way, the box simulates the combustion chamber of the engine in which the electrical resistors generate the released energy. The thermal power chosen is similar to that which would be produced in the real operating conditions of the components to be tested. They simulate the conditions of energy generation by combustion. Thermocouples are placed on the inner and outer surfaces of the system to be tested. Figure 4 shows the installation scheme, and Figure 5 shows photographs of the installation and a detail of the location of thermocouples on the inner surfaces. Thermographs are also taken of the external surfaces, which are the ones visible to the camera. Figure 6 shows thermographs taken from the experiments.

https://doi.org/10.52202/069564-0035

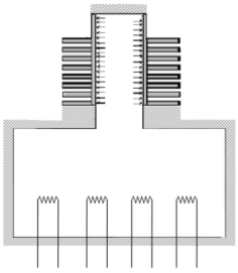

Figure 4. Installation scheme for methodology validation.

Tests were carried out with electrical powers of 150, and 600 W and the cylinder and cylinder head of an air-cooled reciprocating internal combustion engine with finned outer surfaces were chosen as parts. When the temperatures at the thermocouples and the temperature and pressure inside the case reached a steady state, approximately 30 minutes, the thermocouple temperatures and thermographs of all visible surfaces were recorded (Figure 6), and the values of the ambient conditions were also recorded.

3. Selection of the set of boundary conditions

Several sets of boundary conditions can be imposed to estimate the temperature of the inner surface of the cylinder head or cylinder. The proposed ones are:

a) The temperature at the outer surfaces and heat flux at the inner surface.
b) Convective heat transfer coefficient on the outer surfaces and heat flux on the inner surface, such that the temperatures of the outer surfaces match the measured temperatures.
c) The temperature at the outer surfaces and heat flux due to convection at the outer surface.

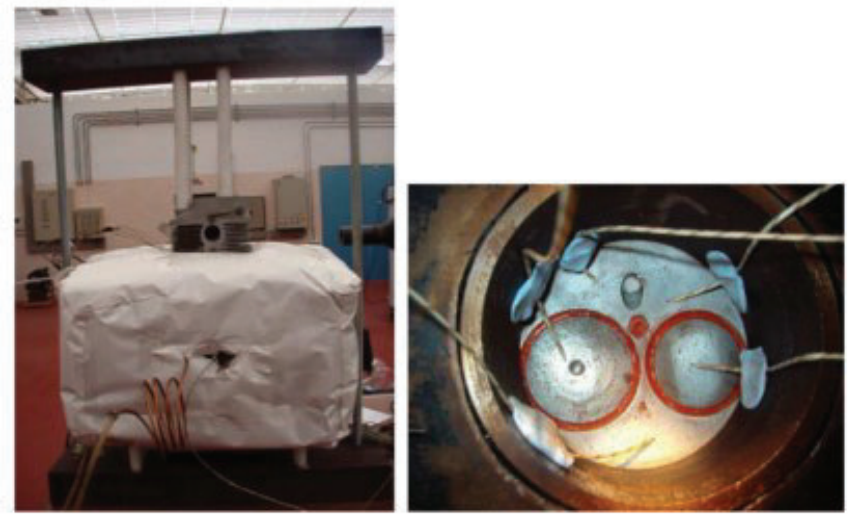

Figure 5. a) Installation setup; b) thermocouples on inner surfaces.

The set of boundary conditions c) is discarded because of the need to impose boundary conditions on all finned surfaces for FEM resolution, which is impossible from a practical point of view.

The two possible sets of boundary conditions, a) and b), are applied to the two chosen components.

3.1 Previous analysis of the boundary conditions

In this case, the set of boundary conditions a) is applied. The external surface temperature field is imposed from the temperature measurements obtained in the test. This field is of the logarithmic type, as shown in Section 2.2:

Step 1: This step intends to obtain a logarithmic-type temperature distribution on the fins by imposing on the bottom and end nodes of the fins the temperatures measured in the test. As discussed in Section 2.2, the errors in the temperature distribution are small regardless of whether a linear or logarithmic distribution is applied. However, the errors in the flow distribution through the surface are relevant. It should be noted that

these are the only boundary conditions applied and that the rest of the surfaces (lateral surface of the fins, inner surface of the cylinder head and non-finned surfaces of the cylinder head) are adiabatic. A scheme of Step 1 is shown in Figure 7.

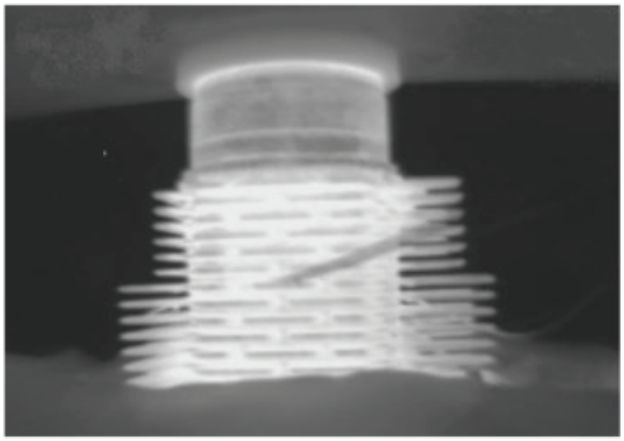

Figure 6. Extended surface cylinder thermograph.

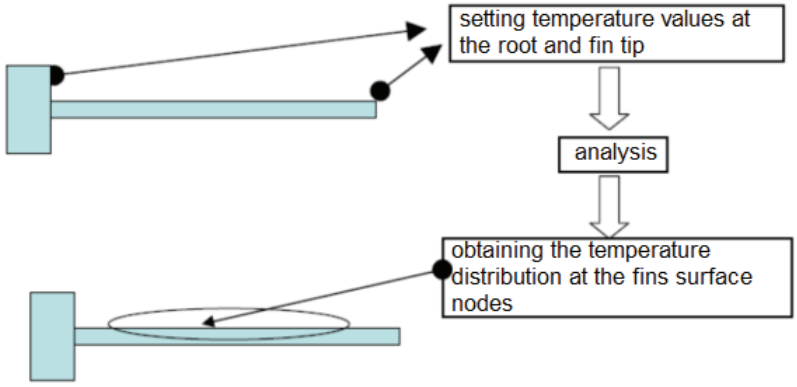

Figure 7. Step 1 of the boundary conditions set election.

Step 2: in this step, the temperatures of the finned surfaces obtained in Step 1 are imposed as a boundary condition; other boundary conditions modelling the test are also imposed, Figure 8:

- heat flow through the inner surface of the cylinder head,
- free convection transfer coefficient from the non-finned outer surfaces to the environment,
- other surfaces are considered adiabatic

3.2. Analysis of the simulation results

The temperature distribution is obtained from the resolution of this model and matches the measured values. However, the heat flux distribution is not valid since it results from solving a one-dimensional conduction problem in the fin in Step 1. This model forces the appearance of local heat fluxes that are transferred from the environment to the root of the fin, called auxiliary fluxes. A scheme of such auxiliary flows is shown in Figure 9. This situation is unrealistic and persists in Step 2 of this resolution and cannot be cancelled.

Therefore, although the temperature field on the outer surfaces is adequate, the heat flux distribution is not. This is the reason why this set of boundary conditions cannot be imposed on the simulation of the cylinder head and cylinder when the engine is under load. The second set of boundary conditions and their validity for the estimation of the average inner surface temperature of the two systems tested is presented below.

In view of the conclusions of the analysis of the application of the set of conditions a), which advise against its use, the set of boundary conditions b), which imposes free convection transfer on the surfaces, is applied. The measured heat power is uniformly distributed on the inner surface.

https://doi.org/10.52202/069564-0035

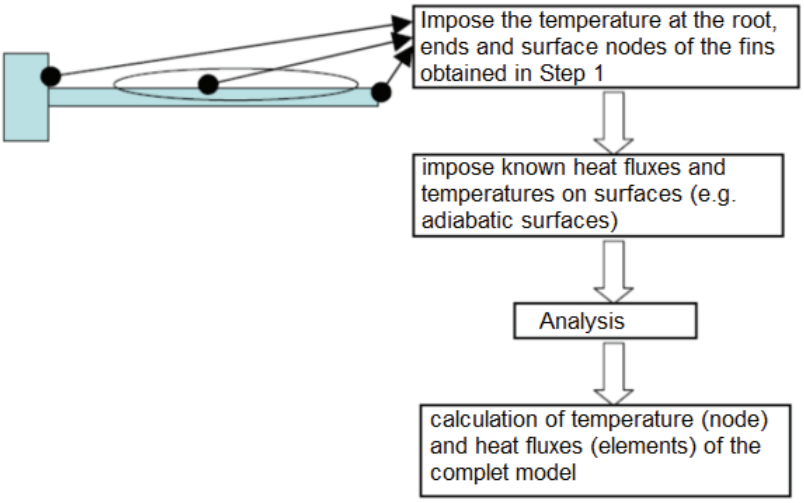

Figure 8. Step 2 of the boundary conditions set election.

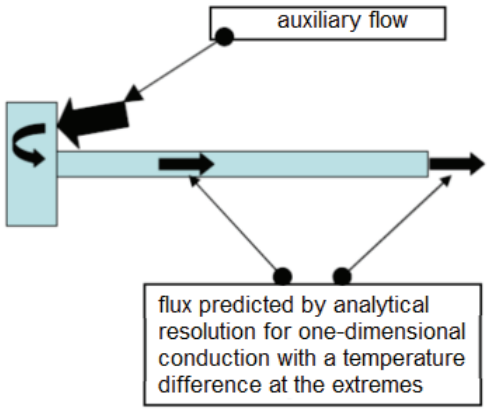

Figure 9. Auxiliary flows representation.

Once the boundary conditions are imposed: uniform heat flux over the elements of the inner surface of the cylinder, which is equal to the heat power generated by the electrical resistors, and the convection coefficient over the elements of the finned surfaces, the model with the applied loads is sent to the NX/NASTRAN solver module.

The temperatures measured on the external surfaces by thermographs and thermocouples will be compared with the temperature field on the external surfaces obtained from the FEM simulation from an initial heat transfer coefficient. If this correspondence does not occur, the comparison is iterated with FEM simulation results with another heat transfer coefficient value.

4. Methodology proposed

A comprehensive review of heat transfer on extended surfaces has been carried out in the previous sections, and the best selection of boundary conditions for temperature determination has been studied. This work aims to determine the average inner surface temperature of systems with extended outer surfaces inside which there is power generation. An inverse method that solves the heat transfer in these systems by means of finite elements is then proposed and described, taking into account the previous considerations exposed in Sections 2 and 3. The main difficulty of this kind of approach is the correct imposition of the boundary conditions in the models and the value of these boundary conditions, whose considerations have been discussed in Section 3. A flow diagram of this methodology is presented in Figure 10.

In the proposed method, the following boundary conditions are chosen:

- Heat flow through the inner walls of the system to the outside, $\dot{Q}_{heat}$

- The heat transfer coefficient on the outer surfaces h_{ext}, which is obtained from an iterative process that converges when the temperatures on the outer surfaces resulting from the FEM model match the measured ones,
- The temperatures of the selected points of the external surfaces and whose values are obtained from the thermographs and those recorded in the thermocouples during the tests, $T_{meas,k}^{outer}$.

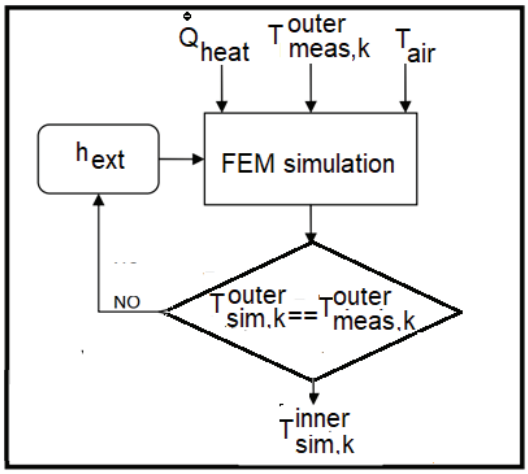

Figure. 10. Methodology flow diagram.

The value of the heat flow through the inner walls of the system, $\dot{Q}_{heat}$, is the heat released by the electrical resistances, whose total value is known but not its distribution along the inner surface. The FEM model requires the heat per unit area and time as a boundary condition. The heat distribution is assumed to be uniform, and the inner surfaces whose outer equivalent are not finned, which is also adiabatic, are considered adiabatic.

The second boundary condition imposed is the convective heat transfer from the outer extended surface to the surrounding air. The heat transfer coefficient h_{ext} is constant and the air temperature is constant.

The cylinder head is an example of those components where there are several parts, and the interaction between surfaces must be considered. In this case, it is considered that the bond between the contact surfaces is perfect and the conductivity is infinite.

Once the boundary conditions have been applied, the model is sent to the NX/NASTRAN solver module.

Once the boundary conditions have been successfully applied, the model is sent to the NX/NASTRAN solver module.

When the simulation is finished, the temperatures of the outer finned surfaces are obtained in the FEMAP post-processing module. Due to the large surface area, points were chosen to compare the measured temperature with the temperature resulting from each simulation. The values of the 9 thermocouples and 10 points on the thermographs were chosen, in total 19 points. The 19 measured temperature values, $T_{meas,k}^{outer}$., are compared with those resulting from the simulation, $T_{sim,k}^{outer}$. k indicates the temperature point being compared. The mean square variation, called MSE, is defined according to Equation (2):

$$MSE = \frac{1}{n}\sum_{k=1}^{k=n}\left(T_{sim,k}^{outer} - T_{meas,k}^{outer}\right)^2, \quad (2)$$

The method attempts to identify the value of h_{ext} that minimizes the mean square error with the temperature measurements MSE_{min}, Figure 11. To calculate such an optimal value of h_{ext} an iterative search process is followed based on interpolations of $MSE(h_{ext})$ as a Cubic Spline type curve. The search is initialized by taking three sufficiently distant values of h_{ext} and calculating the MSE values, they produce.

These $MSE(h_{ext})$ curve values are then interpolated by Spline, and the minimum of the interpolated curve and the corresponding hext,CIL value are calculated. The model is then simulated with this value, and the MSE it produces is calculated. If no significant improvement of MSE is achieved, relative difference below 5%, it is considered to have converged to MSE_{min}. If the improvement is significant, it is incorporated into the interpolation of MSE_{min} by Cubic Spline and iterated again.

As an example, the method when the extended surface cylinder is tested, and the internal thermal generation is equal to 150 kW is illustrated in Figure 12.

https://doi.org/10.52202/069564-0035

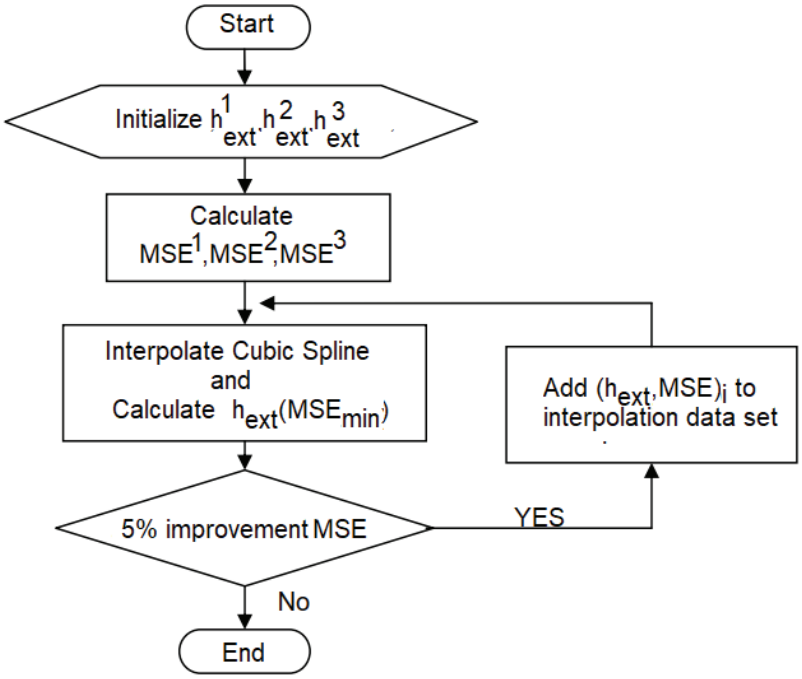

Figure. 11. Heat transfer coefficient iterative method.

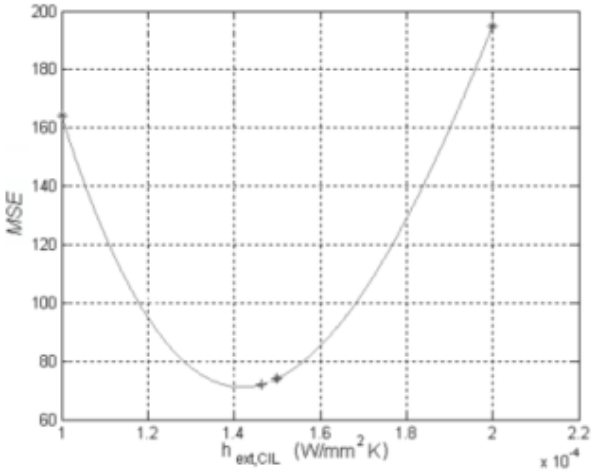

Figure. 12. MSE for different heat transfer coefficients values according to the iteration method

A representation of the temperatures at the chosen points, resulting from experimentation and simulations, for the internal and external surfaces is shown in Figure 13. As can be seen, the difference between the simulation and measured temperatures is quite small. Figure 14 shows a comparison of FEM simulation results with thermography measurements, proving the great similarity between the two.

It is verified that the resulting inner surface temperatures correspond to those measured with thermocouples in the tests. As for the distribution of the heat flows, it is verified that, in all cases, on the whole external surface they are transferred from the environment to the cylinder head and that on the internal surface, the flows are incoming. There are no auxiliary heat flows from the environment to the fins, as in the previous case. The total power transferred through each of the surfaces is also obtained, and it is found that the power transferred through the outer surfaces is equal to that generated by the electrical resistors. It should be noted that the proportion of power transferred to the environment from the finned surfaces is much higher than that associated with the non-finned surfaces. Once this correspondence has been achieved, it is verified that the resulting interior surface temperatures correspond to those measured with thermocouples in the tests.

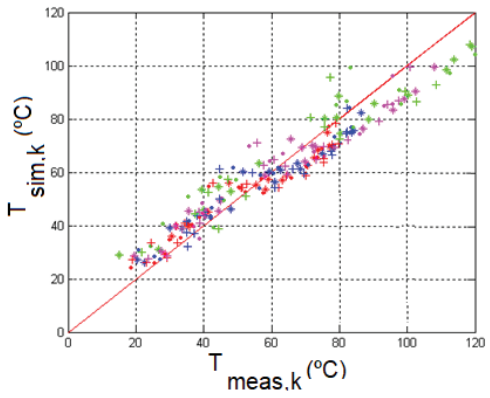

Figure. 13. Representation of temperatures at the points of comparison.

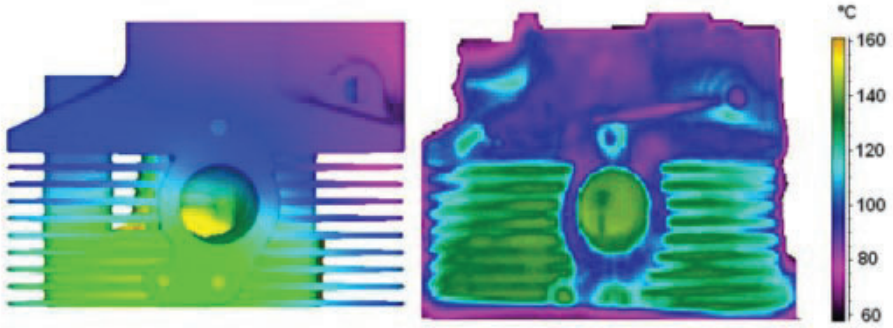

Figure. 14. Comparison of FEM simulation results with thermographs, for tests at 150 W and cylinder head as a component.

5. Conclusions

This work presents a methodology for an accurate evaluation of the inner temperature of high-temperature thermal energy systems. It is developed for being applied to hard-to-monitor systems, such as internal combustion engines or high-temperature energy storage systems. The methodology is demonstrated in an air-cooled internal combustion engine but is fully applicable to any other thermal system with the characteristics described.

Regarding the distribution of the heat flows, it is verified that, for all cases, in all the external surfaces, these are transferred from the environment to the cylinder head and that in the internal surface, the flows are incoming. There are no auxiliary heat flows from the environment to the fins, as in the previous case. The total power transferred through each of the surfaces is also obtained, and it is found that the power transferred through the outer surfaces is equal to that generated by the electrical resistors. It should be noted that the proportion of power transferred to the environment from the finned surfaces is much higher than that associated with the non-finned surfaces.

Therefore, the inverse methodology for determining internal surface temperatures by non-intrusive means has been validated.

Acknowledgments

This work was partially supported by the project MOTHERESE, TED2021-131839B funded by the Spanish Ministry of Science and Innovation and European Union through Plan of Recovery, transformation and resilience funds

References

Journals:

[1] Šarić S, Basara B, Žunič Z. “Advanced near-wall modeling for engine heat transfer”. Int J Heat Fluid Flow 2017; 63:205–211.

https://doi.org/10.52202/069564-0035

[2] Irimescu A, Merola SS, Tornatore C, Valentino G. “Development of a semi-empirical convective heat transfer correlation based on thermodynamic and optical measurements in a spark ignition engine”. Appl Energy 2015; 157:777–788.

[3] Bürkle, Sebastian, et al. "In-cylinder temperature measurements in a motored IC engine using TDLAS." Flow, Turbulence and Combustion 2018; 101: 139-159.

[4] Rieker, G. B., Li, H., Liu, X., Liu, J. T. C., Jeffries, J. B., Hanson, R. K., .& Takatani, S. “Rapid measurements of temperature and H2O concentration in IC engines with a spark plug-mounted diode laser sensor”. Proceedings of the Combustion Institute 2007; 31(2), 3041-3049.

[5] Birkigt, A., Michels, K., Theobald, J., Seeger, T., Gao, Y., Weikl, M. C., ... & Leipertz, A. “Investigation of compression temperature in highly charged spark-ignition engines”. International Journal of Engine Research 2011; 12(3), 282-292.

[6] Finol, C. A., and K. Robinson. "Thermal modelling of modern engines: a review of empirical correlations to estimate the in-cylinder heat transfer coefficient." Proceedings of the institution of mechanical engineers, part D: journal of automobile engineering 2006; 220.12: 1765-1781.

[7] Catto A. G., Prata A. T., A numerical study of instantaneous heat transfer during compression and expansion in piston-cylinder geometry. Numerical Heat Transfer Part A 2000; 38:281-303.

[8] Huang, Cheng-Hung, and Chien-Tsuen Lee. "An inverse problem to estimate simultaneously six internal heat fluxes for a square combustion chamber." International Journal of Thermal Sciences 2015; 88: 59-76.

[9] Bohac, Stanislav V., Douglas M. Baker, and Dennis N. Assanis. "A global model for steady state and transient SI engine heat transfer studies." SAE transactions 1996: 196-214.

[10] Jing, Dong Zhan, and Wei Gang Zheng. "A Numerical Simulation of steady-state temperature field of natural gas engine piston." Applied Mechanics and Materials. Vol. 496. Trans Tech Publications Ltd, 2014.

[11] Fonseca, Leonardo, et al. "Internal combustion engine heat transfer and wall temperature modeling: an overview." Archives of Computational Methods in Engineering 2000; 27.5: 1661-1679.

[12] Liu, Yong, and R. D. Reitz. "Modeling of heat conduction within chamber walls for multidimensional internal combustion engine simulations." *International Journal of Heat and Mass Transfer* 1998; 41.6-7): 859-869.

[13] Cerdoun, Mahfoudh, Carlo Carcasci, and Adel Ghenaiet. "Analysis of unsteady heat transfer of internal combustion engines exhaust valves." International Journal of Engine Research 2018; 19.6: 613-630.